APPENDIX A

AERIAL PHOTOGRAPH INTERPRETATION

A1. INTRODUCTION

The geomorphological features within the site (defined as the catchment of Landslides A to D), interpreted from the 1949 and 1999 aerial photographs, are shown on Figure A1. All recorded landslides, both recent and relict, are also shown on this figure. Minor landslides are labelled A1, A2 etc. Figure A2 shows details of the mining activities in the vicinity of Landslide C (based on the 1949 aerial photographs), and Figure A3 shows the details of the geomorphology and interpretative observations in the vicinity of Landslide B (based on the low-level 1973 aerial photographs). Figure A4 shows the extent of hillfires identified from all available aerial photographs.

A2. DETAILED OBSERVATIONS

YEAR	OBSERVATIONS
1945	Single, high-level poor quality photograph. The photo does not cover the source areas of Landslides B and C. Mining works to the east of the site are clearly visible. The ‘fresh’ appearance of the disturbed ground suggests that mining activity may have been comparatively recent at the time the photograph was taken (the nature of the mining works is described in detail below).
1949	With the exception of occasional graves, minor footpaths and cultivated fields in the valley floor, the western end of the site is generally undeveloped and consists of natural hillside. However, the eastern end of the site is extensively disturbed as a result of what appears to be surface strip mining (Figure A2). The mining appears to involve surface excavation, presumably along the mineralised quartz veins that traverse the hillside, and shows up as in a series of discontinuous sub-parallel cut slopes running east-northeast to west-southwest across the natural hillside. The cut slopes appear to be typically between 1 m and 3 m high. Below the cut slopes are irregular lightly coloured areas that are interpreted to be accumulations of fill (tailings) excavated during the mining of the quartz veins and end tipped downslope. Large quantities of fill are also visible within DC6. Extensive areas of sheet and gully erosion are visible within the fill bodies. In addition, a number of what appear to be adits, generally located on the same alignment as the cut slopes, are visible. Elongated lobes of fill are located below these adits. Downhill of the mining works are two relatively large cut and fill platforms together with a number of smaller cut platforms. Abandoned and generally derelict structures, presumably industrial buildings used for ore processing, are located on these platforms. Various footpaths connect the buildings with the mining operations. While the mine appears abandoned, the lack of vegetation on the areas of fill and cut slopes indicates work may only recently have ceased, possibly within 5 years or so prior to the photographs being taken. Away from the mined area, the natural hillside is sparsely vegetated, with occasional areas of small shrubs/trees located within the natural drainage lines. Paddy fields cover the base of the valley to the southeast of the site; the fields

YEAR	OBSERVATIONS
	become terraced in the gently inclined ground at the toe of the hillside. No recent failures are visible on the natural hillside within the site. However, as previously mentioned, extensive areas of sheet and deep gully erosion are visible within the fill bodies. A cluster of relict landslide scars is visible on the northeast flank of DC6 (49A to 49G). The failures appear to have been relatively large (~100 m^3) and are mostly located below an area of exposed rock. Many areas of surface erosion are visible on the natural hillside (Figure A1). These areas are generally restricted to along the ridgeline forming the northwest boundary of the site and uphill of minor footpaths that traverse the hillside.
1963	Many one-storey, probably residential buildings, have been constructed within the valley to the southeast of the site, scattered amongst the cultivated fields. The area under cultivation has also increased with the development of terraced fields on the lower hillside. Various structures, some apparently industrial, have been constructed on the platforms in the vicinity of the mining works. A new track has also been constructed along the toe of the hillside. A number of graves are visible on the lower flanks of DC2 and DC3. Much of the hillside remains thinly vegetated, though on the lower hillside parallel rows of trees/shrubs have been planted. Vegetation cover on the areas of fill remains sparse. No recent failures are visible on the natural hillside. However, extensive areas of sheet and gully erosion remain visible within the fill. Local areas of surface erosion or possibly minor failures are also visible on some of the mining cut slopes. Prominent boulder fields are visible within the rounded natural drainage lines in the west of the site (DC1 and DC1B). These may originate from relict channelised debris flow deposits, though no definable scars are visible. The areas of natural surface erosion along the ridgelines are still clearly visible.
1964	The track that traverses the toe of the hillside has been extended to the west. Branches from the track terminate at the base of DC1 and DC2. Ground disturbance within and above these channels suggests some sort of quarrying/mining activity, possibly the surface excavation of quartz (quartz veins are visible in this area).
1973	Many more one-storey residential structures have been constructed on the previously cultivated land at the floor of the valley. Some of the surrounding fields are no longer under cultivation. Numerous recently constructed graves are visible in the vicinity of DC2 and DC3. Much of the lower section of the hillside has become densely vegetated, though the areas of fill are still sparsely vegetated. The upper section of the hillside is still thinly vegetated with grass, with an increasing number of small trees/shrubs mostly found within the natural drainage lines.

YEAR	OBSERVATIONS
	No recent failures are visible within the site. The fill shows signs of only minor recent surface erosion, though the previously eroded gullies are clearly visible. This low level photographs clearly shows the ground conditions at the locations of Landslides B and C. LANDSLIDE B (Figure A3) A lozenge shaped body of what appears to be colluvium (bouldery ground apparently overlying exposed rock) is visible below the exposed rock cliff to the west of natural drainage line DC3. A second accumulation of colluvium consisting of angular boulders is visible within the adjacent natural drainage line to the west (DC3B). Close to the head of the drainage line is what appears to be a minor recent failure, with a gully leading directly from this failure into the drainage line below. It is considered likely that this represents a natural seepage (spring). The possible spring is located within the source area of Landslide B. A minor natural drainage concentration is visible along the centre line of the source area of the landslide. A prominent steeply inclined cliff of exposed granite is visible directly above the source area. A series of parallel west to east trending persistent photogeological lineaments (probably sheeting joints) traverse the exposed rock cliff face. Sparse vegetation is visible along these lineaments. A single curved lineament (fault?), with a broadly northwest to southeast trend cuts (and appears to displace) these parallel features and appears to run towards the location of the source of Landslide B. Dense vegetation is visible along parts of this feature indicating possible seepage. LANDSLIDE C. The mining cut slope along which Landslide C occurred appears higher, possibly by 2 m to 3 m, than the adjacent mining cut slopes. The crest of the slope in plan forms a partly crenulated boundary, probably as a result of numerous juxtaposed minor failures and local areas of erosion on the slope. Irregular lobes of fill, marked by the absence of vegetation, and bouldery ground occur below the cut slopes. In places, the cut slopes have been exposed to past concentrated surface water flows resulting in the formation of erosion gullies both in the fill and natural ground. To the west of the source area is a rounded depression from which a poorly defined natural drainage line forms. An irregular area of exposed rock forming a minor cliff is located above the source area. Regular photogeological lineaments visible on the cliff are probably associated with jointing. A second exposure of rock is visible in the drainage line below the source area (a retaining wall located on this rock exposure, noted in the July 2000 site inspection, has yet to be constructed).
1977	There is little visible change to the residential or agricultural developments to the southeast of the site. Many of the footpaths that crossed the hillside are no longer visible, presumably having become revegetated through disuse. The vegetation of the hillside to the east of the site appears significantly thinner. It is not possible to infer if this is as a result of seasonal drought or hillfires.

YEAR	OBSERVATIONS
	Fresh areas of disturbance visible on the cut slopes adjacent to the source area of Landslide C are probably due to surface erosion rather than failures of the slope.
1979	A linear track, part of the site preparation works for the installation of pylons to support overhead cables, traverses the base of the hillside. Light coloured patches over most of the middle and upper section of the hillside, including the source areas of Landslides B and C, probably indicate the extent of a recent hillfire (Figure A4). No evidence of recent landslides.
1980	Twin lines of pylons are under construction towards the base of the natural hillside. The areas around the base of each pylon have been cleared of vegetation. Many of the fields to the southeast of the site appear to be no longer under cultivation. No evidence of recent landslides.
1980	The upper line of pylons has been completed. The lower line is still under construction. No evidence of recent landslides.
1982	High level photographs with only partial coverage of the site. Many of the residential properties to the southeast of the site have been demolished. Earthworks, as part of the construction for Leung King Estate, have commenced within the valley to the southeast of the site. A minor, recent open hillside type failure is visible on the natural hillside between DC3 and DC3A (NTLI Reference No. 9). Two further failures are also visible on the northeast flank of DC4 (82A and 82B). Both these failures are likely to have occurred within fill bodies formed during the earlier mining works.
1983	Extensive earthworks have commenced affecting the whole of the floor of the valley. All visible structures and previously cultivated fields have been demolished. The cut slopes that border the southeast of the site are under construction. Evidence of a recent hillfire is visible at the western end of the site.
1984	Earthworks are ongoing. Staining visible on the lower part of the partially excavated cut slopes above Leung King Estate is probably due to seepage.
1985	Site preparation work appears to be largely complete. Local areas of minor erosion, probably due to seepage, are visible on the recent cut slope.

YEAR	OBSERVATIONS
	An area of pale coloured ground, due to a minor hillfire, is visible at the eastern end of the site (Figure A4). Where the vegetation has been burnt, the gullies within the fill are clearly visible. A single recent failure (85A) is visible above the recently excavated cut slope on the west flank of DC4.
1985	A pale disturbed area of vegetation indicating a recent hillfire is visible on the southwest flank of DC6
1986	A crib wall (Slope No. 5SE-B/R5) is under construction at the base of the cut slope (Slope No. 5SE-B/CR26) above Leung King Estate. Much of the hillside has been affected by a major hillfire. As a result of removal of the vegetation cover, linear zones of pale surface coloration leading from the areas of erosion along the ridgelines, down the natural drainage lines are clearly visible. These features on the NTLI are shown (incorrectly) as debris trails. A minor open hillside type failure (86A) is visible on the natural hillside between DC3 and DC3B
1987	The construction of Leung King Estate is ongoing. The areas of erosion on the mining cut slope adjacent to the source area of Landslide C are no longer visible.
1988	Construction of Leung King Estate is ongoing; otherwise there is no visible change.
1991	Construction of Leung King Estate is complete. Construction of an adjacent DSD pumping station is ongoing. A minor road is also under construction along the southwest boundary of the site Much of the hillside has been affected by a large hillfire; the fire affected the source area of Landslide B (Figure A4). A number of failure scars are visible within the site (Figure A1): • 91A- a relatively large failure above the road under construction, • 91B- a minor failure at the head of DC1A, • 91C and 91D- a pair of minor failures on the flanks of the natural drainage line which marks the southwest boundary of the site. The failures are located below an area of exposed rock, and • 91E and 91F- a pair of failures on the southwest flank of DC6. The debris from the larger of these failures has become channelised.
1992	Partial coverage of the site. Construction of the DSD pumping station is ongoing and construction of the minor

YEAR	OBSERVATIONS
	road appears complete. Otherwise there is no visible change.
1993	Construction of the DSD pumping station is complete. A hillfire has affected the natural hillside to the northeast of DC6 (Figure A4). A landslide scar (93A) is visible at the same location as the 1991 failure (91B) at the head of DC1A.
1994	A recent partially channelised failure is visible on the northeast flank of DC1 (94A). Otherwise there is no visible change.
1996	An area of previously natural hillside adjacent to the southwest boundary of the site is under cultivation. Otherwise there is no visible change.
1996	Evidence of minor recent hillfires visible adjacent to DC1 and to the northwest of DC6 (Figure A4). Otherwise there is no visible change.
1998	A prominent channelised failure visible at the head of DC1A (98A). The debris has accumulated within a relatively level area below a rock exposure.
1998	High level poor quality photographs. Damage from a minor hillfire is visible at the southwest boundary of the site (Figure A4).
1999	The vegetation on the cut slope at the boundary of Leung King Estate has been cut back. Otherwise there is no visible change.
1999	No visible significant change.

A3. AERIAL PHOTOGRAPHS

Year	Aerial Photograph Reference No.	Altitude (feet)
1945	Y00629	20000
1949	Y01833, Y01834	Unknown
1963	Y09206, Y09207, Y09283, Y09284	3900
1964	Y11709, Y11710, Y11711	Unknown
1973	4198, 4199, 4200	1500
1973	6748, 6749, 6750	2500
1977	19580, 19581	4000
1979	25134, 25135, 25136	4000
1980	33147, 33148	4000

Year	Aerial Photograph Reference No.	Altitude (feet)
1980	30620, 30621	5500
1982	44604, 44605	10000
1983	51935, 51936, 51937	4000
1984	54085, 54086	4000
1985	A00212, A00213	4000
1985	A02334, A02335	4000
1986	A04822, A04823, A04824	4000
1987	A09726, A09727	4000
1988	A13930, A13931	4000
1991	A27232, A27233	4000
1992	A31288, A31289	4000
1993	A35245, A35246	4000
1994	A39859, A39860	4000
1996	CN13471, CN13472	6000
1996	CN16494, CN16495	3500
1998	CN20399, CN20400	4000
1998	CN21510, CN21511	8000
1999	CN24817, CN24818	4000
1999	A49076, A49077	4000

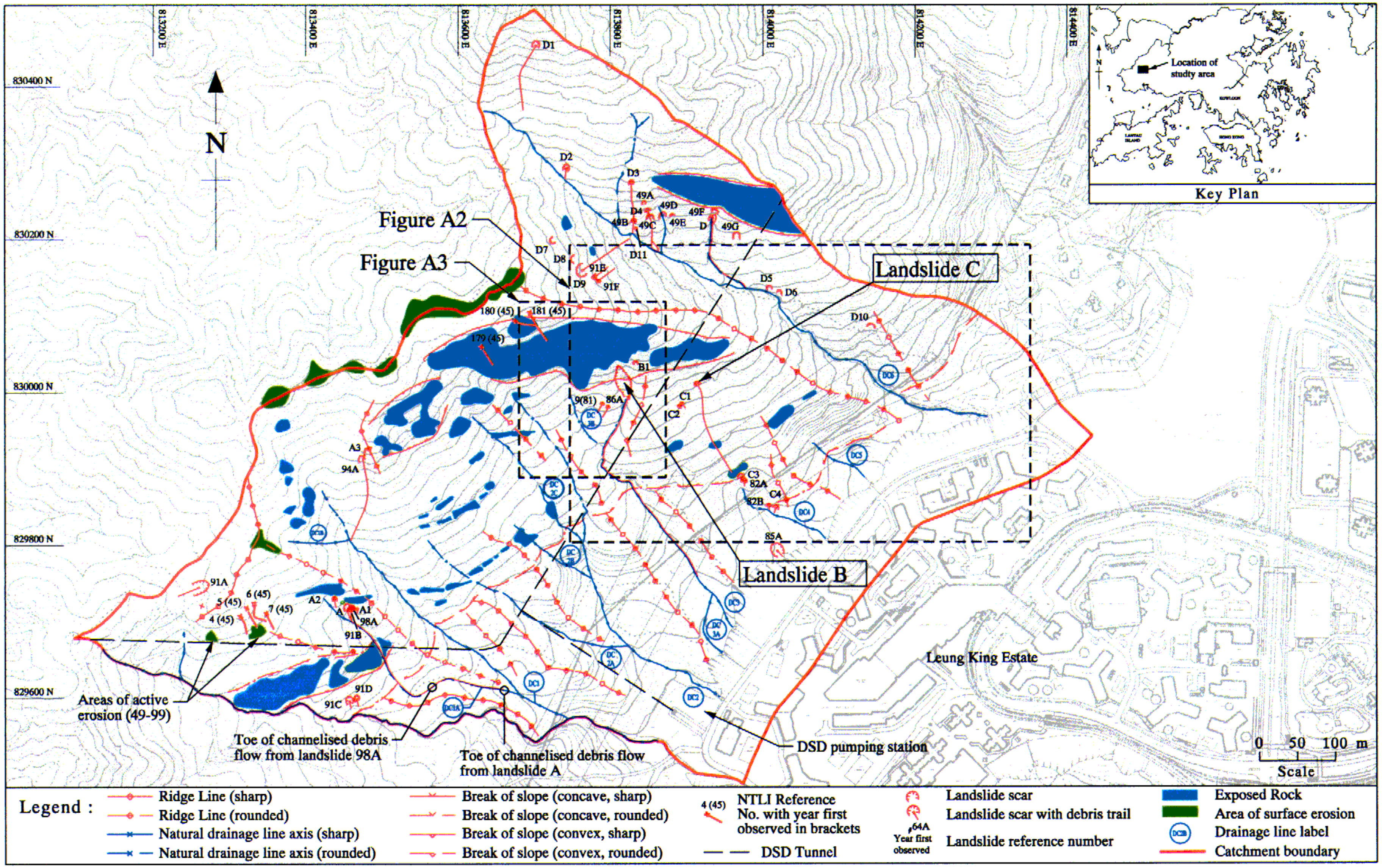

Figure A1 - Aerial Photograph Interpretation of the Study Area (Based on Photographs taken between 1949 and 1999)

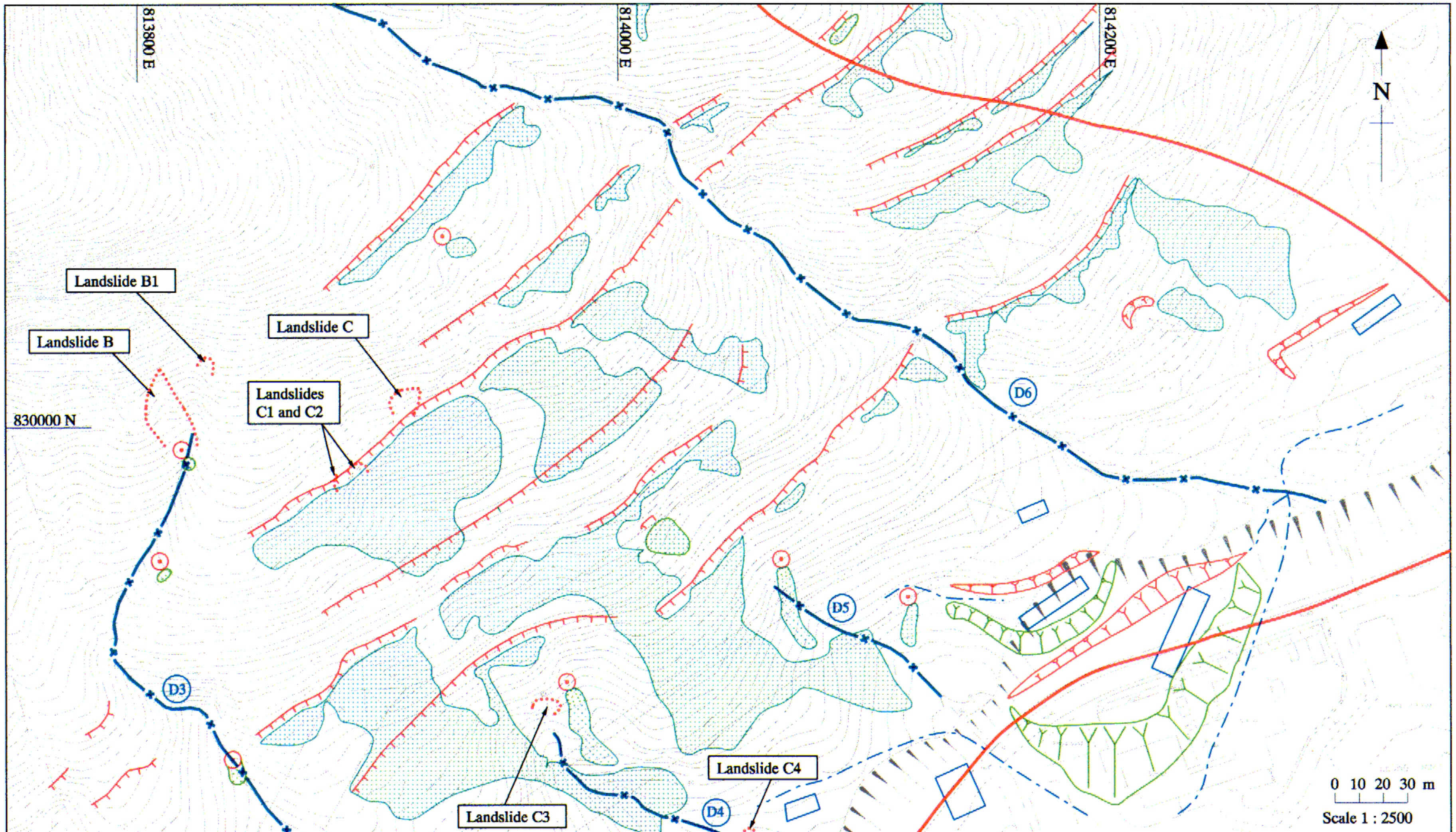

Legend : Excavated slope; Adits; Mining waste; Fill slope; Cut slope; Track; Natural drainage line; Building

Note : Plan geometry is based on Topographic Survey Drawing No. GCS 2837 (Survey Division, CED, 2000), Sheet No. 5SE-5A and site measurement.

Figure A2 - Aerial Photograph Interpretion of the Area of Mining (Based on Photographs taken in 1949)

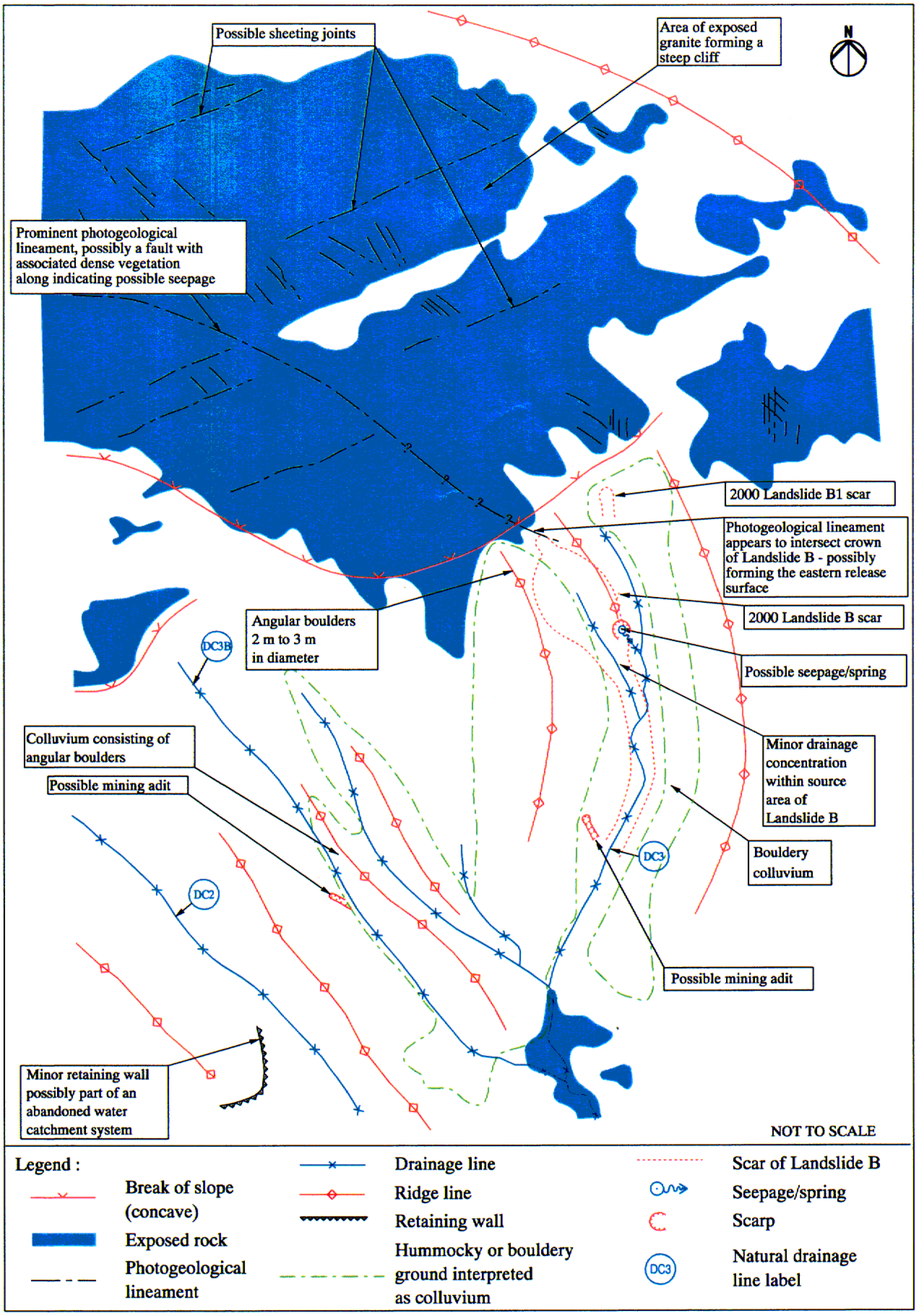

Figure A3 - Detailed Aerial Photograph Interpretation in the Vicinity of Landslide B
(Based on Photographs taken in December 1973)

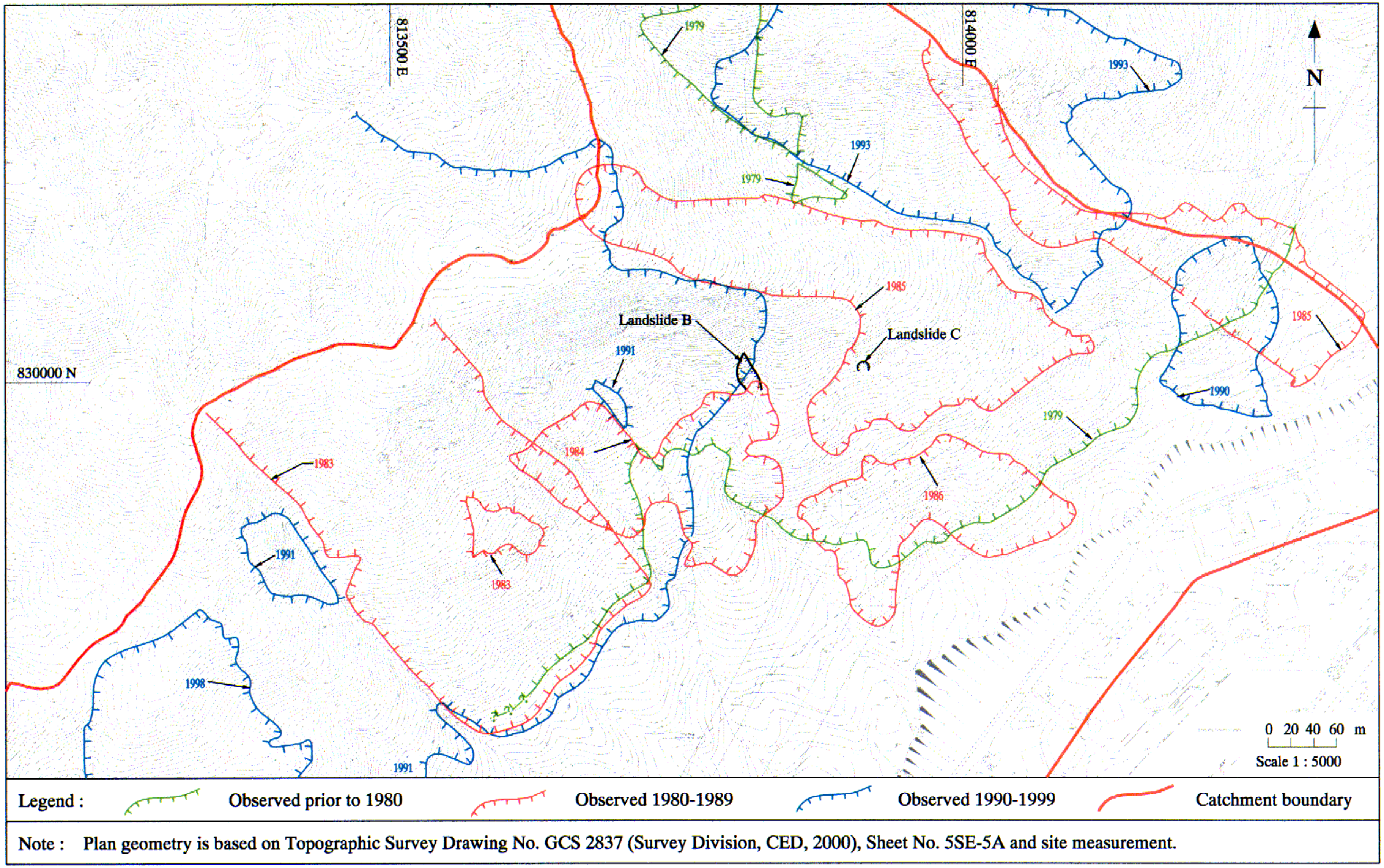

Figure A4 - Location of Hillfires within Study Area (Based on Aerial Photographs taken between 1949 and 1999)

APPENDIX B

ESTIMATES OF VOLUMES OF LANDSLIDES B AND C

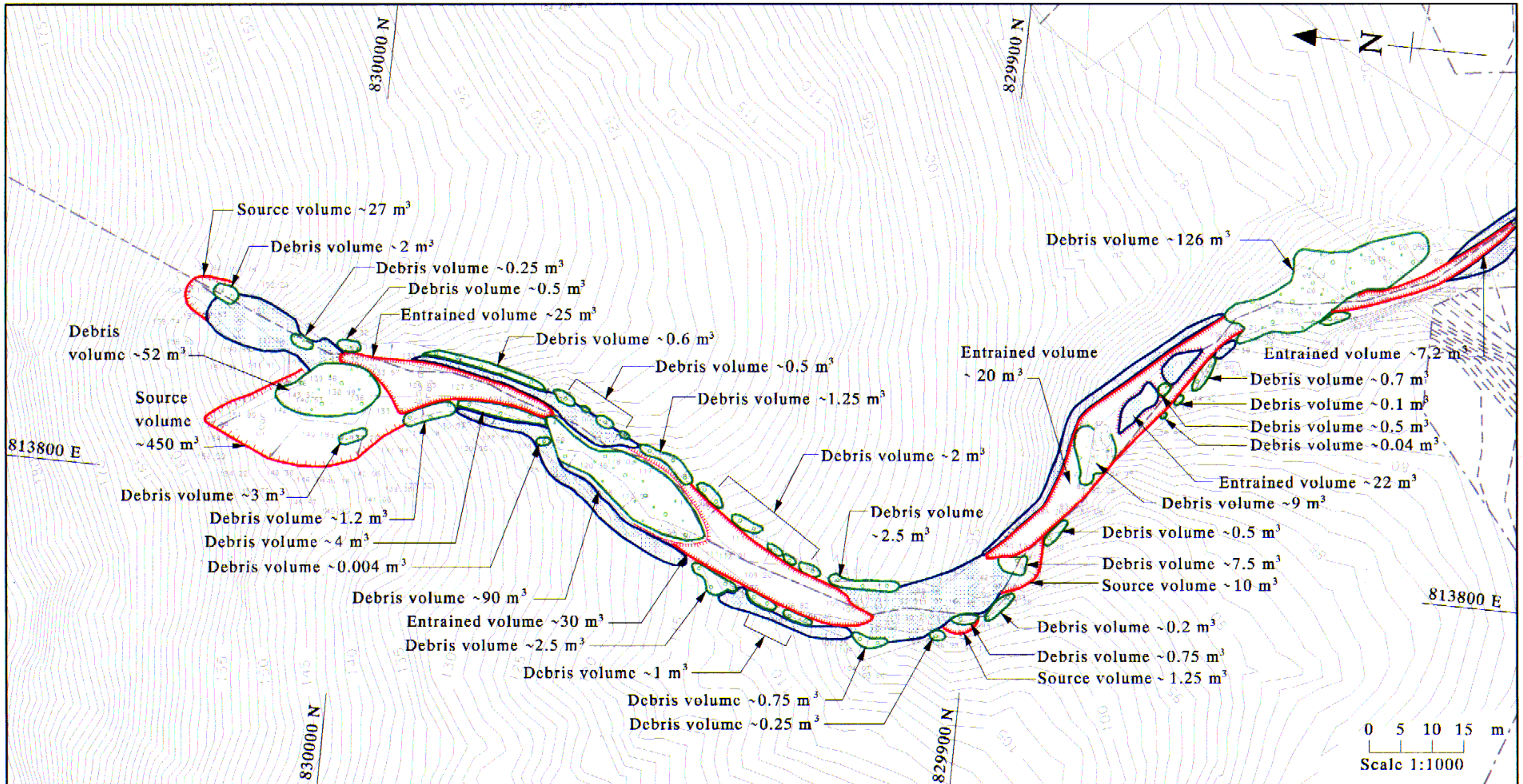

Legend : Main scarp; Zone of erosion; Chainage; Line of section; Zone of transportation; Zone of deposition

Note : Plan geometry is based on Topographic Survey Drg GCS 2837 (Survey Division, CED, 2000), Sheet No 5SE-5A and site measurement.

Figure B1 - Plan of Upper Section of Debris Trail for Landslide B Showing Source, Debris and Entrained volume

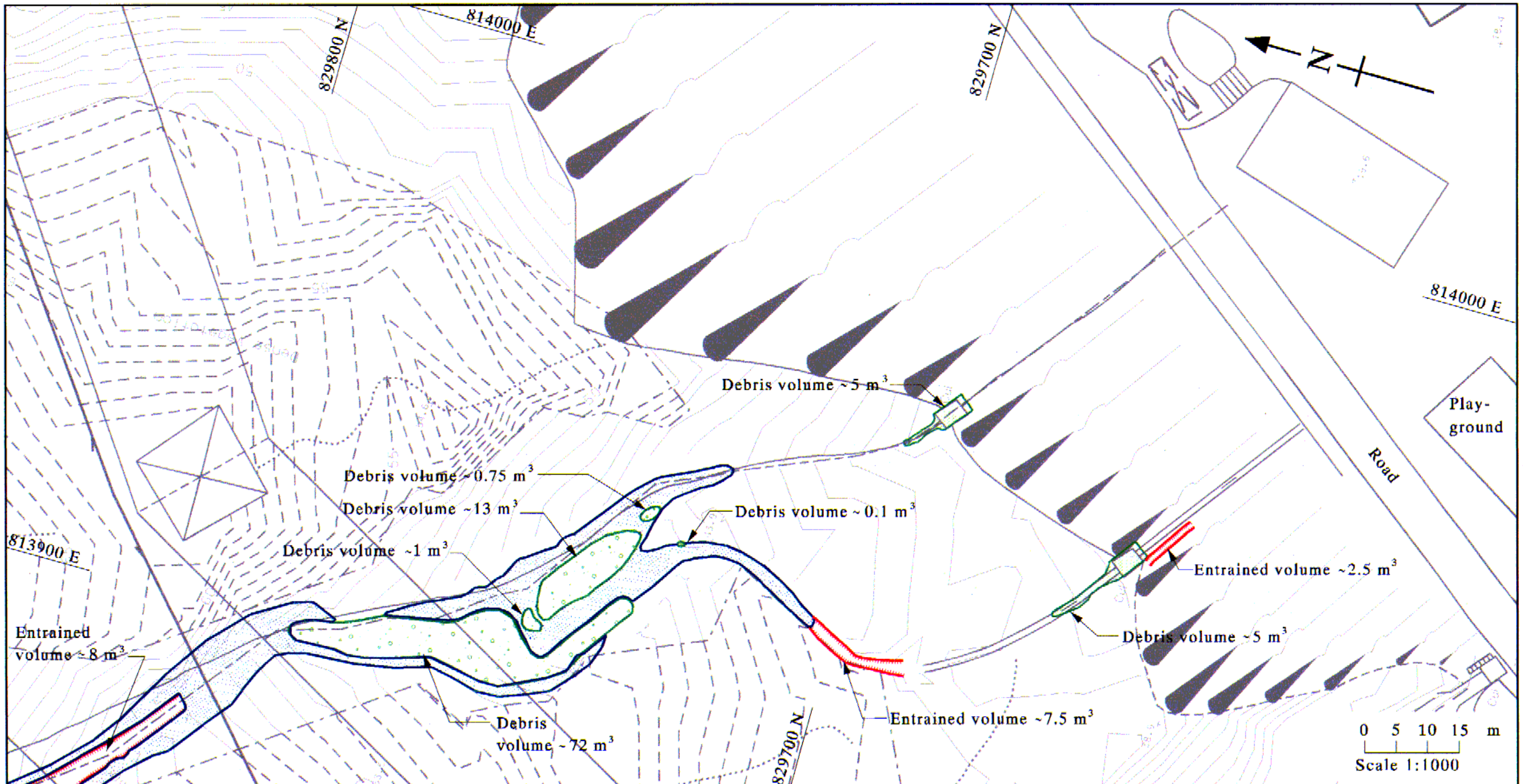

Note : Plan geometry is based on Topographic Survey Drg GCS 2837 (Survey Division, CED, 2000), Sheet No 5SE-5A and site measurement.

Figure B2 - Plan of Lower Section of Debris Trail for Landslide B Showing Source, Debris and Entrained Volume

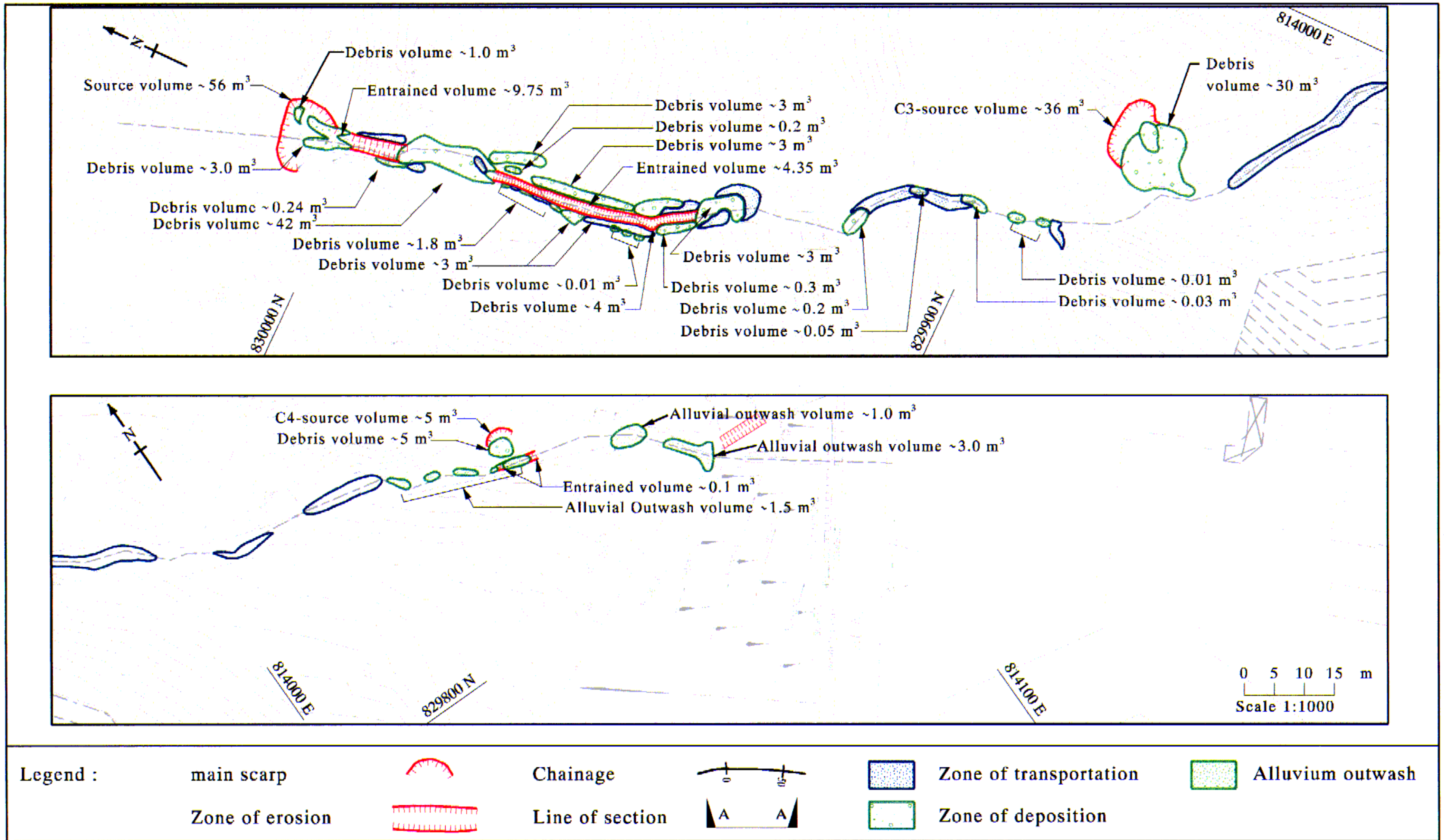

Note : Plan geometry is based on Topographic Survey Drg GCS 2837 (Survey Division, CED, 2000), Sheet No 5SE-5A and site measurement.

Figure B3 - Plan of the Debris Trail for Landslide C Showing Source, Debris and Entrained Volume

APPENDIX C

THEORETICAL STABILITY ANALYSIS

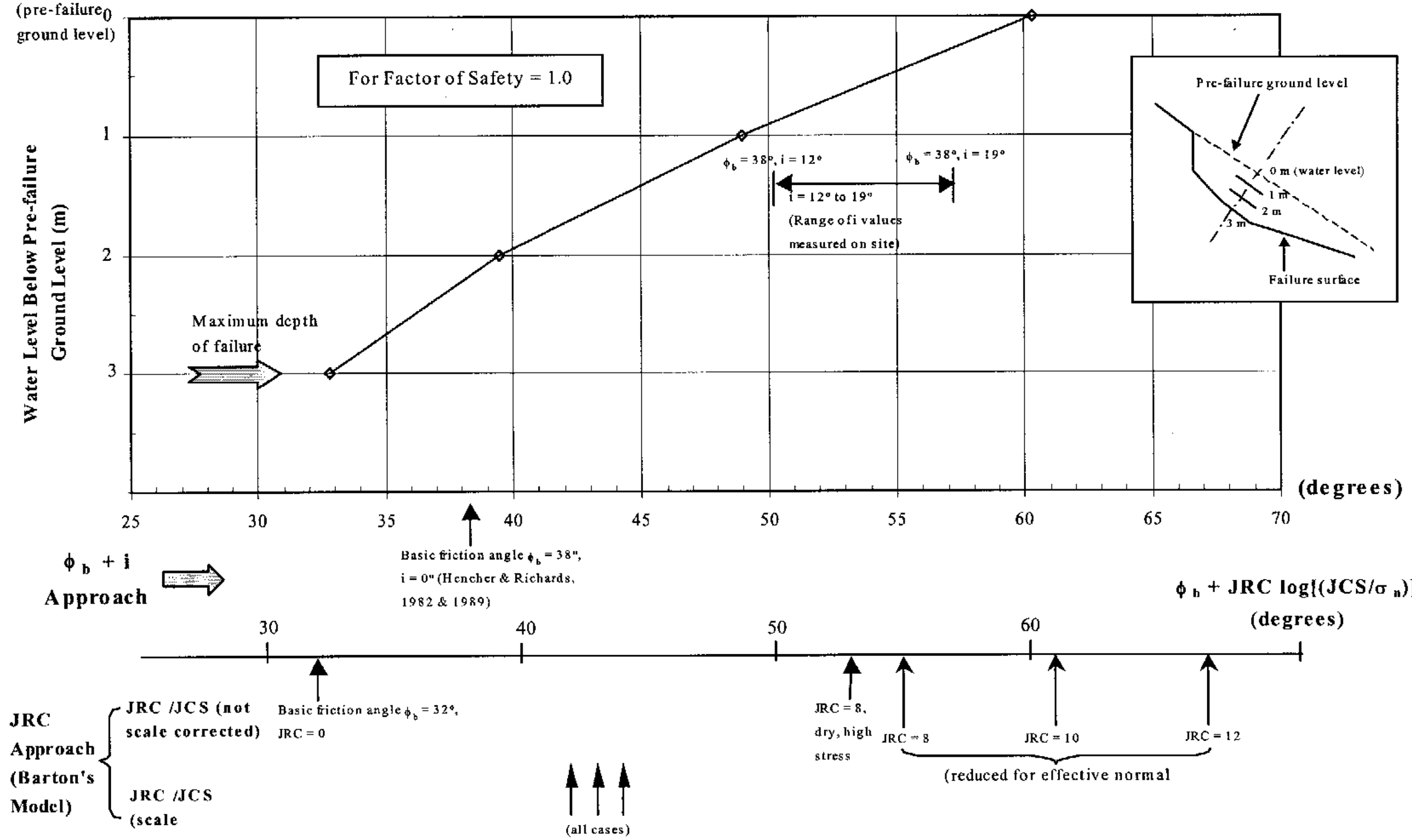

Note: (1) Refer to Section A-A in Figure 6.
(2) Water levels are measured from pre-failure ground level down to failure surface (illustrated in above small figure).
(3) JRC approach is based on Barton's equation (ref. Barton, 1990). Detailed calculations refer to Appendix C.

Figure C1 - Nomogram of Water Level Versus Shear Strength for Factor of Safety = 1.0 at Landslide B

HALCROW CALCULATION SHEET	Page: 1 of 2	Rev:
Project : Detailed Study at Leung King Estate	By: E Ren	Date: 11-Jan-01
Subject : Stability analysis- joint surface roughness using JRC approach	Checked By: D Andrews	Date: 12-Jan-01

1. Shear strength of rough surfaces

A natural discontinuity surface in hard rock is never as smooth as a sawn or ground surface of the type used for determining the basic friction angle. The undulations and asperities on a natural joint surface have a significant influence on its shear behaviour. Generally, this surface roughness increases the shear strength of the surface, and this strength increase is extremely important in terms of stability.

Based on Patton's saw-tooth specimens, the shear strength can be represented as follows:

$\tau = \sigma_n \tan(\phi_b + i)$ .... (1)

where ϕ_b is the basic friction angle of the surface and
i is the angle of the saw-tooth face

References / Results
Book title :
"Support of Underground Excavations in Hard Rock" by E Hoek, P K Kaiser & W F Bawden, 1995

2. Barton's model

Barton and his co-workers (1973, 1976, 1977, 1990) have studied the behaviour of natural rock joints in great detail and have proposed that equation (1) can be re-written as:

$\tau = \sigma_n \tan[\phi_b + JRC \log(JCS/\sigma_n)]$ .... (2)

From above equation (1) and (2), i can be derived as follows:

$i = JRC \log[JCS/\sigma_n]$ .... (3)

where JRC is the joint roughness coefficient and
JCS is the joint wall compressive strength, σ_n is the total normal stress

3. Scale effects on shear strength estimation

The roughness terms $(JRC)_o$ and the logarithmic strength/stress ratio represent a stress - and roughness-dependent value for i. A further improvement to this (i) value estimation was the introduction of size-dependent JRC and JCS values, termed JRC_n and JCS_n.

Based on Barton's paper " Scale effects or sampling bias?" (1990), the approximate equations for estimating JRCn and JCSn at larger scale are as follows:

$JRC_n = JRC_o(L_n/L_o)^{-0.02JRCo}$ .... (4)

$JCS_n = JCS_o(L_n/L_o)^{-0.03JRCo}$ .... (5)

Where L_o = laboratory size joint samples (nominal 100mm)
L_n = natural block size

Book title :
" SCALE EFFECTS IN ROCK MASSES" edited by A. Pinto Da Cunha

4. Using the JRC approach to calculate roughness angle for Landslide B at Leung King Estate (Not corrected for scale)

Use the cross section A-A of Landslide B in Figure 6 of Detailed Study Report

Assume γ = 20 kN/m^3 JCS_o = 20 MPa ϕ_b=32° (ref. Barton, 1993)
JRC_o = 8 to 12 Z = 3 m (assumed average depth measured from pre-failure ground level)
Average slope angle = 35 degrees

1) Assumed water table at pre-failure ground level, then the effective normal stress (σ_n') :

$\sigma_n' = \gamma' \times z \times \cos 35°$ = ((20 - 9.8)*3)*COS(35*PI()/180) = 25 kPa

a) If JRC_o = 8, then $i = JRC_o \log[JCS_o/\sigma_n']$ = 23 degrees $\phi_b + i = 32 + 23 = 55°$
b) If JRC_o = 10, then $i = JRC_o \log[JCS_o/\sigma_n']$ = 29 degrees $\phi_b + i = 32 + 29 = 61°$
c) If JRC_o = 12, then $i = JRC_o \log[JCS_o/\sigma_n']$ = 35 degrees $\phi_b + i = 32 + 35 = 67°$

using equation (3)

2) Assumed water table below slip surface (i.e. dry condition),

$\sigma_n = \gamma' \times z \times \cos 35°$ = ((20 - 0)*3)*COS(35*PI()/180) = 49 kPa

a) If JRC_o = 8, then $i = JRC_o \log[JCS_o/\sigma_n]$ = 21 degrees $\phi_b + i = 32 + 21 = 53°$
b) If JRC_o = 10, then $i = JRC_o \log[JCS_o/\sigma_n]$ = 26 degrees $\phi_b + i = 32 + 26 = 58°$
c) If JRC_o = 12, then $\iota = JRC_o \log[JCS_o/\sigma_n]$ = 31 degrees $\phi_b + i = 32 + 35 = 63°$

using equation (3)

HALCROW CALCULATION SHEET	Page: 2 of 2	Rev:
Project : Detailed Study at Leung King Estate	By: E Ren	Date: 11-Jan-01
Subject : Stability analysis- joint surface roughness using JRC approach	Checked By: D Andrews	Date: 12-Jan-01

5. Using the JRC approach to calculate roughness angle for Landslide B at Leung King Estate (Corrected for scale)

Use the cross section of Landslide B (see Figure 6 for section A-A, detailed study report)

Assume $r =$ 20 kN/m^3 $JCS_o =$ 20 MPa $\phi_b = 32^\circ$ (ref. Barton, 1993)

$JRC_o =$ 8 to 12 $Z =$ 3 m (assumed average depth measured from pre-failure ground level)

Average slope angle = 35 degrees, Natural block size about 4m

1) Assumed water table at pre-failure ground level, then the effective normal stress (σ_n') :

$\sigma_n' = \gamma' \times z \times \cos 35^\circ$ = ((20 - 9.8)*3)*COS(35*PI()/180) = 25 kPa

a) If $JRC_o = 8$, then
$JRC_n = JRC_o(L_n/L_o)^{-0.02JRCo} = 8\,(4/0.1)^{-0.02*8}$ = 4.4 — using equation (4)
$JCS_n = JCS_o\,(L_n/L_o)^{-0.03JRCo} = 20\,(4/0.1)^{-0.03*8}$ = 8.3 MPa — using equation (5)
$i = JRC_n \log [JCS_n/\sigma_n']$ = 11 degrees $\phi_b + i = 32 + 11 = 43^\circ$ — using equation (3)

b) If $JRC_o = 10$, then
$JRC_n = JRC_o(L_n/L_o)^{-0.02JRCo} = 10\,(4/0.1)^{-0.02*10}$ = 4.8
$JCS_n = JCS_o\,(L_n/L_o)^{-0.03JRCo} = 20\,(4/0.1)^{-0.03*10}$ = 6.6
$i = JRC_n \log [JCS_n/\sigma_n']$ = 12 degrees $\phi_b + i = 32 + 12 = 44^\circ$

c) If $JRC_o = 12$, then
$JRC_n = JRC_o(L_n/L_o)^{-0.02JRCo} = 12\,(4/0.1)^{-0.02*12}$ = 5.0
$JCS_n = JCS_o\,(L_n/L_o)^{-0.03JRCo} = 20\,(4/0.1)^{-0.03*10}$ = 5.3
$i = JRC_n \log [JCS_n/\sigma_n']$ = 12 degrees $\phi_b + i = 32 + 12 = 44^\circ$

2) Assumed water table below slip surface (i.e. dry condition), then the total normal stress (σ_n) :

$\sigma_n = \gamma' \times z \times \cos 35^\circ$ = ((20 - 0)*3)*COS(35*PI()/180) = 49 kPa

a) If $JRC_o = 8$, then
$JRC_n = JRC_o(L_n/L_o)^{-0.02JRCo} = 8\,(4/0.1)^{-0.02*8}$ = 4.4
$JCS_n = JCS_o\,(L_n/L_o)^{-0.03JRCo} = 20\,(4/0.1)^{-0.03*8}$ = 8.3 MPa
$i = JRC_n \log [JCS_n/\sigma_n]$ = 10 degrees $\phi_b + i = 32 + 10 = 42^\circ$

b) If $JRC_o = 10$, then
$JRC_n = JRC_o(L_n/L_o)^{-0.02JRCo} = 10\,(4/0.1)^{-0.02*10}$ = 4.8 — using equation (4)
$JCS_n = JCS_o\,(L_n/L_o)^{-0.03JRCo} = 20\,(4/0.1)^{-0.03*10}$ = 6.6 — using equation (5)
$i = JRC_n \log [JCS_n/\sigma_n]$ = 10 degrees $\phi_b + i = 32 + 10 = 42^\circ$ — using equation (3)

c) If $JRC_o = 12$, then
$JRC_n = JRC_o(L_n/L_o)^{-0.02JRCo} = 12\,(4/0.1)^{-0.02*12}$ = 5.0
$JCS_n = JCS_o\,(L_n/L_o)^{-0.03JRCo} = 20\,(4/0.1)^{-0.03*10}$ = 5.3
$i = JRC_n \log [JCS_n/\sigma_n]$ = 10 degrees $\phi_b + i = 32 + 10 = 42^\circ$